Evolution of a large-periodicity soliton lattice in a current-driven electronic crystal

V. L. R. Jacques,[1,2,3,*] D. Le Bolloc'h,[2] S. Ravy,[3] J. Dumas,[4] C. V. Colin,[4] and C. Mazzoli[5,1]

[1]*European Synchrotron Radiation Facility, 6 rue Jules Horowitz, BP 220, F-38043 Grenoble cedex, France*

[2]*Laboratoire de Physique des Solides (CNRS-UMR 8502), Bâtiment 510, Université Paris-sud, F-91405 Orsay cedex, France*

[3]*Synchrotron SOLEIL, L'Orme des Merisiers, Saint-Aubin BP 48, F-91192 Gif-sur-Yvette cedex, France*

[4]*Institut Néel, CNRS and Université Joseph Fourier, F-38042 Grenoble, France*

[5]*Dipartimento di Fisica, Politecnico di Milano, Piazza L. Da Vinci 32, I-20133 Milano, Italy*

(Received 21 October 2011; revised manuscript received 18 December 2011; published 17 January 2012)

We report here on a detailed coherent x-ray diffraction study of the charge-density wave in $K_{0.3}MoO_3$ as a function of an external current. At threshold current, the charge-density wave undergoes a strong decrease of average amplitude keeping large correlation lengths. At the same time, an extra electronic modulation with large periodicity appears directly related to the sliding of the charge-density wave. This effect is interpreted as the formation of a soliton lattice and its evolution with respect to external current is investigated. The charge-density wave phase is found to undergo an anharmonic to harmonic transition when a current is injected.

DOI: 10.1103/PhysRevB.85.035113 PACS number(s): 71.45.Lr

The collective motion of electrons has always been a fascinating topic in condensed-matter physics. In charge-density wave (CDW) systems, transport measurements were the first to provide a clear signature of the collective motion of condensed electrons.[1] A nonlinear conductivity is observed above a threshold current I_T and is attributed to depinning of the CDW on impurities.[2,3] An excess current then arises as well as a broadband noise and current oscillations.[4] Although the electron-density modulation involved in CDWs is very small, x-ray diffraction provides information about the structure of the CDW as it is associated with a periodic lattice distortion. These atomic displacements give rise to two satellite reflections at twice the Fermi wave vector $2k_F$ from each fundamental Bragg peak. The intensity and profile of these reflections can thus be studied as a function of external current. Because the diffracted intensity does not depend on the CDW phase with respect to the lattice, the sliding of the CDW *as a whole* is in principle invisible by diffraction techniques. But some studies on blue bronze $K_{0.3}MoO_3$ (Refs. 5 and 6) and $NbSe_3$ (Refs. 7–11) evidenced clear diffraction effects under current, all due to the presence of intrinsic or extrinsic defects. The CDW was, for instance, found to lose its transverse coherence above threshold,[5,6] and to have a different wave vector close to the contacts[8,9] or near crystal steps.[10,11]

In a recent paper,[12] we reported on another feature observed in the sliding regime: for large currents, secondary satellites appear in the close vicinity of the CDW reflections. The period of the corresponding modulation is in the micrometer range, i.e., 1000 times larger than the CDW period ($\lambda_{CDW} = \frac{2\pi}{2k_F} \sim$ 10 Å). Such long-range electronic correlations are unprecedented in electronic systems. In the following, we report on a careful analysis of this effect as a function of external current.

The use of a high-resolution setup together with a coherent beam is mandatory to access very fine structures in reciprocal space associated to such large periodicities in real space. The experiment was performed at the ID20 beamline of ESRF.[13] A 7.6 keV beam was selected by a double Si(111) monochromator providing a $\Delta\lambda/\lambda = 1.4 \times 10^{-4}$ bandpass, fixing the longitudinal coherence length to 0.8 μm.[12] The beam size was reduced to 200 μm with slits located after the optics and 10 m upstream of the sample, leading to a transverse coherence length ~8 μm at sample position. Well-polished slits opened at 10 μm were inserted 10 cm before the sample to select the coherent part of the beam. A 22 μm pixel size charge-coupled device (CCD) camera located 1.76 m downstream of the sample was used for detection. Within this experimental setup, the resolution is $\Delta q = 0.8 \times 10^{-4}$ Å^{-1} and the total degree of coherence reaches 18%.[14]

$K_{0.3}MoO_3$ (blue bronze) is a typical quasi-one-dimensional system made of parallel chains of MoO_6 clusters, aligned along the [010] direction ($b = 7.56$ Å) in a monoclinic C lattice ($\beta = 117.5°$), and forming layers in the ($\boldsymbol{b}$, $\boldsymbol{a} + 2\boldsymbol{c}$) plane.[15] The Fermi surface is composed of two pairs of slightly warped sheets perpendicular to the chains, allowing a nesting with wave vector $\boldsymbol{q}_{2\boldsymbol{k}_F} \approx 0.748\ \boldsymbol{b}^*$.[16] Due to Coulomb repulsion between adjacent chains in the $\boldsymbol{c}$ direction, the CDW wave vector $\boldsymbol{q}_s = (1, 2k_F, \overline{0.5})$ is not parallel to the nesting wave vector $\boldsymbol{q}_{2\boldsymbol{k}_F}$. The electron density reads

$$\rho(\boldsymbol{r}) = \rho_0 \left[1 + \frac{\Delta}{\hbar v_F k_F \Lambda} \cos\left[\boldsymbol{q}_s \cdot \boldsymbol{r} + \Phi(\boldsymbol{r})\right]\right] + \frac{e}{\pi} \nabla \Phi(\boldsymbol{r}), \tag{1}$$

where $\rho_0 = 2e$, Δ is the electronic gap value, v_F and k_F are the Fermi velocity and wave vector, respectively, Λ is a constant related to the electron-phonon coupling, and $\Phi(\boldsymbol{r})$ is the CDW phase whose space dependence will be used later.

The CDW of blue bronze is incommensurate with the underlying lattice, allowing it to slide when submitted to a current larger than a threshold current I_T. Above I_T, the dV/dI versus I curve displays an abrupt change of slope and voltage oscillations are observed.[17] Moreover, crystal defects (impurities, dislocations, nonstoichiometry) or nonuniform contact resistance are responsible for an inhomogeneous current flow through the sample.[18]

A high quality single crystal, $5 \times 3 \times 0.5$ mm^3 in size, was mounted into a top-loading He flow cryostat and cooled down to 70 K with 1 mK accuracy, below the Peierls temperature ($T_c = 180$ K). Four linear silver contacts were deposited perpendicularly to the chains axis [see sketch in Fig. 1(j)]. The two outer contacts were used for current injection, and

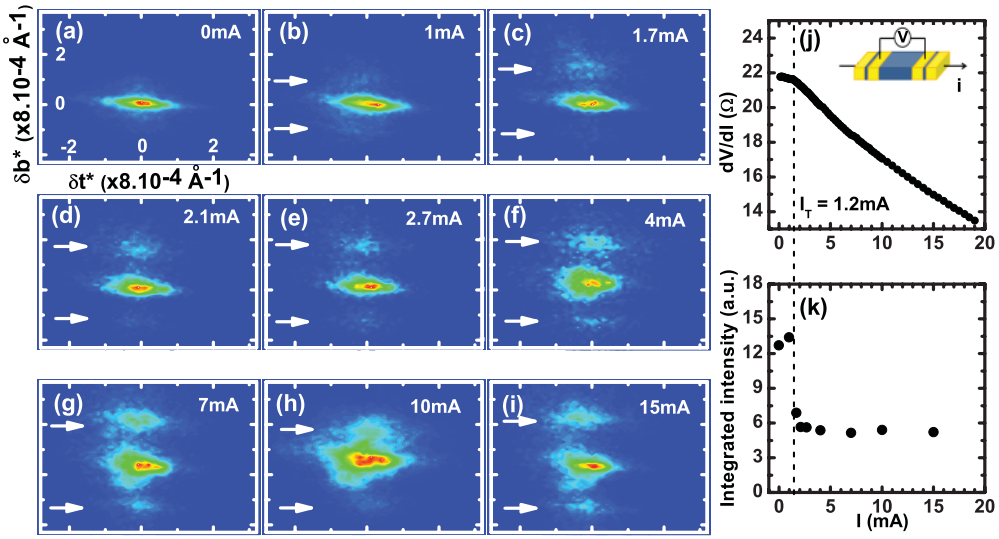

FIG. 1. (Color online) (a)–(i) Projection of the recorded three-dimensional (3D) intensity around the CDW reflection onto the CCD plane ($\boldsymbol{b}^*$,$\boldsymbol{t}^*$) at different currents, and $T = 70$ K. $\delta\boldsymbol{b}^*$ and $\delta\boldsymbol{t}^*$ refer to the relative distance from the CDW reflection along $\boldsymbol{b}^*$ and $\boldsymbol{t}^*$ respectively. The fields of view along $\boldsymbol{b}^*$ and $\boldsymbol{t}^*$ are the same for each map. The intensity color scale is logarithmic and goes from blue for lowest intensities to red for strongest intensities for each map. (j) dV/dI curve measured during the experiment. (k) Plot of the integrated intensity as a function of current. The dashed line indicates the threshold current value.

the two inner ones to measure the voltage. Transport and diffraction measurements were performed simultaneously. The measured dV/dI curve is plotted in Fig. 1(j) and nonlinear conduction appears at $I_T = 1.2$ mA. After each current cycle, the virgin state was restored by heating the sample up to room temperature for 1 h.

The $\boldsymbol{Q}_s = (5,\bar{1},\bar{3}) + \boldsymbol{q}_s$ satellite reflection has been measured with an incident beam located hundreds of microns away from the electrical contacts. It is one of the most intense satellite reflection at relatively small angles.[19] The incident beam angle is $\theta_i = 12.5^\circ$ and the diffracted one is $\theta_f = 26.4^\circ$. As described in Ref. 12, the diffracted intensity was measured in a small reciprocal volume around $\boldsymbol{Q}_s$ as a function of external current. Figures 1(a)–1(i) show the projection of the central part of this volume onto the ($\boldsymbol{b}^*$,$\boldsymbol{t}^*$) reciprocal plane defined by the CCD camera cut for different currents.

The transverse direction $\boldsymbol{t}^*$ is the horizontal direction of the CCD camera. It is perpendicular to $\boldsymbol{b}^*$ and makes an angle of $\sim 20^\circ$ with respect to $\boldsymbol{2a}^* - \boldsymbol{c}^*$ in reciprocal space. The full width at half maximum (FWHM) along $\boldsymbol{t}^*$ is approximately constant and corresponds to correlations lengths of ~ 500 nm. Along $\boldsymbol{b}^*$, the $\boldsymbol{Q}_s$ FWHM also remains constant with increasing current. The integrated intensity of the 3D patterns are displayed versus current in Fig. 1(k). A strong decrease of intensity occurs at I_T.

Very interesting features appear in the sliding direction $\boldsymbol{b}^*$ and are studied in detail here. The projection of the 3D distribution of intensity onto $\boldsymbol{b}^*$ is displayed in Fig. 2(a). The CDW reflection slightly moves with current but is less than $\pm 10^{-4}$ Å^{-1}.

Beyond the clear intensity decrease with current, and as already reported in Ref. 12, secondary satellites appear at positions $\boldsymbol{Q}_s \pm \boldsymbol{\delta q}$ where $\boldsymbol{\delta q}$ ranges from 0.0005 to 0.001 $\boldsymbol{b}^*$. These were observed several times in different samples but it is noteworthy that some samples do not exhibit this effect. To our point of view this is related to the amount of defects in some samples leading to local inhomogeneities of the CDW. The samples in which the effect was measured were also not homogeneously displaying the secondary satellites. That is why we think that defects must have an influence on the appearance of this phenomenon. A faint sign of the effect is present at 0 mA but is attributed to a nonvirgin state remaining after previous current injections, blue bronze being well known to display memory effects.[20] At $I = 1$ mA, slightly below I_T, they are located in the tail of the $\boldsymbol{Q}_s$ satellite. With increasing current, the secondary satellites continuously move away from $\boldsymbol{Q}_s$. The corresponding wave vector magnitude $\boldsymbol{\delta q}$ as well as the corresponding periodicity $d = 2\pi/\delta q$ versus current are displayed in Figs. 2(b) and 2(c). d decreases from 1.2 μm at I_T to 0.7 μm at 4 mA, and then saturates for larger currents. The secondary satellites FWHM is larger than that of $\boldsymbol{Q}_s$ for $I \leqslant 4$ mA but for higher currents the widths of the secondary satellites and of $\boldsymbol{Q}_s$ are identical. A crucial point for the interpretation of the phenomenon is to note that the two secondary satellites located at $\pm\boldsymbol{\delta q}$ do not have the same intensity, especially for small currents.

To understand these observations, let us first emphasize that the secondary satellites appear for currents close to I_T, which is a strong indication that the effect is induced by the CDW motion. It is also consistent with the fact that no speckle has ever been recorded despite the use of a coherent beam, meaning that the CDW motion leads to a dynamical averaging of the speckles.

Two models can be proposed to account for the appearance of such secondary satellites, either a periodic modulation of the CDW amplitude ρ_0 or of its phase $\Phi(\boldsymbol{r})$. In the former case, the CDW motion would induce 1 μm CDW stripes with modulated amplitudes along $\boldsymbol{b}^*$. Such a pattern would give rise to $\pm\boldsymbol{\delta q}$ secondary satellites but with similar intensities, in contradiction with the observed data. Strong disorder effects could

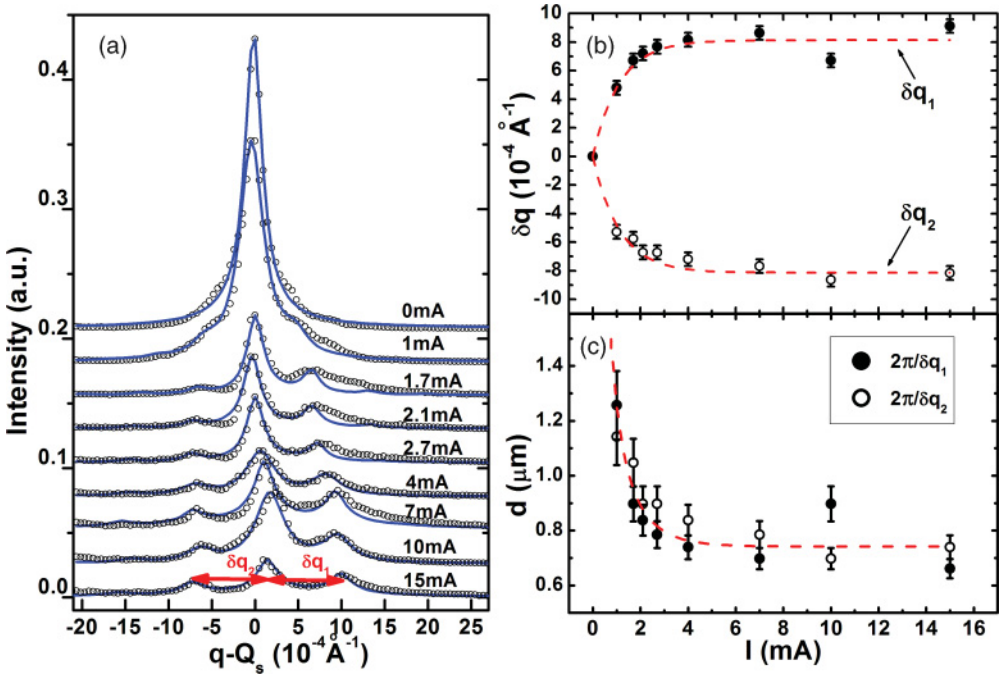

FIG. 2. (Color online) (a) Projection of the CDW reflection along b^* versus current (open circles). The solid lines are fit with the periodic solitonlike sawtoothed function shown in Fig. 3. δq_1 and δq_2 are the distances between the two secondary satellites and the $2k_F$ position. (b) Evolution of δq_1 and δq_2 with external current. (c) Periodicity d obtained from δq_1 (open circles) and δq_2 (black circles) as a function of current. The dashed lines in (b) and (c) are guide to the eyes.

induce the observed intensity asymmetry through a Debye-Waller-like factor, but the distortions necessary to reproduce our measurements are too large to be actually considered.

On the other hand, a simple periodic phase $\Phi(\boldsymbol{r})$ naturally leads to $\pm\boldsymbol{\delta q}$ peaks with asymmetric intensities provided it is not an even function of space. [It can be shown that if x_0 can be found so that $\Phi(x - x_0)$ is an even function of space, then $I(\boldsymbol{q} + \delta\boldsymbol{q}) = I(\boldsymbol{q} - \delta\boldsymbol{q})$.] To explain the occurrence of secondary satellites, the theory of discommensurations is often invoked.[21,22] It states that the modulation wave vector locks in to a commensurate value in large domains to gain the energy of interaction between the host lattice and the modulation. These domains are separated by discommensurations (or solitons), where the elastic energy is lost, and phase changes by $2\pi/p = \pi\alpha$, where p is the order of commensurability.[23] Note that in the case of a CDW, a soliton carries a charge αe. In order to retrieve the actual incommensurate wave value, the domain periodicity d must satisfy

$$d = \pi\alpha/\delta, \tag{2}$$

where δ is the deviation to commensurability. In blue bronze the simplest and closest commensurate wave vector is $(3/4)b^* \approx 2k_F$, which implies that the order of commensurability is $p = 8$ ($\alpha = 1/4$) because $8 \times (1,3/4,\overline{0.5}) = (8,6,\overline{4})$ is a reciprocal wave vector [as first emphasized in Ref. 28, $4\boldsymbol{Q}_s \sim (4,3,\overline{2})$ is not a reciprocal vector of the C lattice]. In the present case $\delta = 3/4 - 2k_F = 0.002b^*$, which leads to $d = 0.05\ \mu$m. With such a periodicity, the secondary satellites would appear 20 times further from the $2k_F$ reflection than observed. Moreover, δq increases with current, which cannot be interpreted within the discommensuration model without changing α, i.e., the position of the CDW reflection. The fact that the CDW still slides is also hardly consistent with the existence of locked in commensurate regions.

A semiphenomenological phase model is presented here, in which the CDW is allowed to make any phase jump, and deform to be in any incommensurate state. The fact that the $2k_F$ satellite reflection does not move indicates that the number of condensed electrons is kept constant, i.e., $\int \nabla\Phi(\boldsymbol{r})d^3\boldsymbol{r} = 0$, which is satisfied if the phase is a periodic function of space. Along the chains (y direction), the following function accounts for a soliton lattice:

$$\Phi(y) = \frac{\pi\alpha}{d}y - \sum_n 2\alpha tg^{-1}[e^{(y-nd)/l_0}] \tag{3}$$

in which d is the observed periodicity. The phase amplitude change $\pi\alpha$ and the soliton length l_0 are free parameters. Note that the discommensuration model is a particular case of that one with $\alpha = 1/4$. The phase profiles giving the best fit to the data and the evolution of α and l_0 with current are displayed in Figs. 3(a) and 3(b). The corresponding calculated diffraction patterns are plotted in Fig. 2(a). The fit is in very good agreement for $I \geqslant 4$ mA, but some discrepancies appear at lower currents.

To illustrate the transverse ordering of the solitons, the CDW is depicted in Fig. 4 for different currents. This structure is in agreement with the fact that the secondary satellites appear purely along b^*, meaning that the solitons form planes perpendicular to the chains. This is indeed the most energetically favorable configuration as it prevents a huge Coulomb repulsion between out-of-phase neighboring chains.

For currents below 4 mA, an inhomogeneous CDW motion could be responsible for the discrepancy between the fitted and measured secondary satellites widths. In this regime,

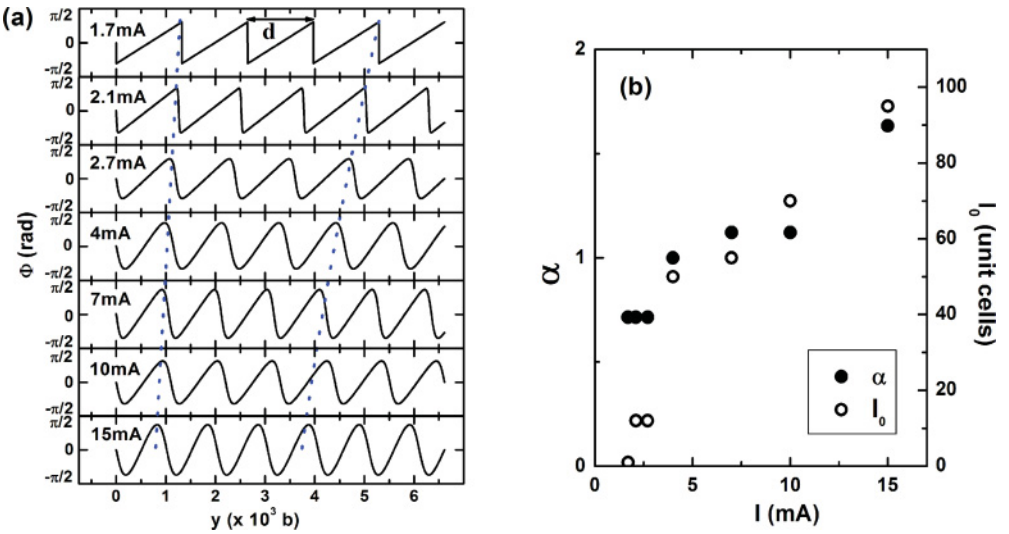

FIG. 3. (Color online) (a) Evolution of the sawtoothed functions versus currents above I_T. The evolution of d is emphasized with the dotted lines. (b) Evolution of α and l_0 with respect to current.

it is indeed well established that some domains begin to slide while others are still pinned.[18] As a consequence, some regions display a certain periodicity of their phase while others have a different one. The summation of several periodicities leads to broader secondary satellites on the average but does not affect the width of the $2k_F$ satellite reflection, as observed. At higher currents, the discrepancy between $2k_F$ and secondary satellite widths is not measured anymore, which is a strong indication that the sliding becomes more homogeneous around 4 mA.

Finally, the integrated intensity of the CDW and secondary satellites dramatically drops at I_T, and this has always been observed at I_T. This puzzling effect does not go together with a sizable broadening of the CDW reflection. Thus the average amplitude of the CDW decreases when it slides, which can be explained by two mechanisms. Either the global amplitude of the CDW decreases everywhere, or the CDW disappears in some regions of the sample, while the remaining regions keep the same correlation length. As the CDW is not homogeneous in the whole sample the second explanation might be more appropriate.

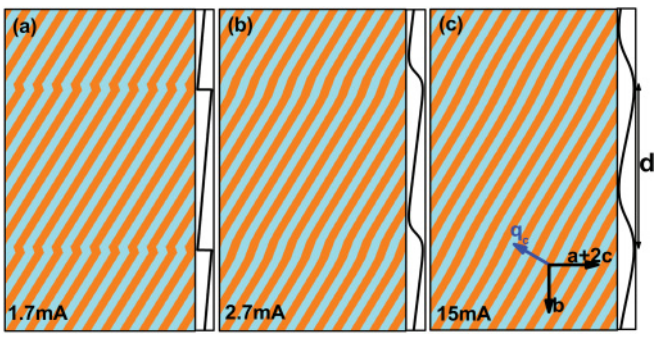

FIG. 4. (Color online) 2D representation of the soliton lattice. The orange (dark gray) to cyan (light gray) scale represents the amplitude of the CDW modulation at 1.7, 2.7, and 15 mA. For clarity, the CDW period is not to scale with the soliton lattice period. The phase profile corresponding to each current is shown on the right of each panel. At 1.7 mA (respectively 2.7 and 15 mA), $d = 1.27$ μm (respectively 0.78 and 0.7 μm).

The present model well accounts for the behavior of the driven CDW in blue bronze but the energetical issue has to be discussed. In the case of the static discommensuration model, the elastic energy loss is compensated by the gain in CDW to lattice coupling. Here, the energy cost of the phase defects formation has to be attributed to external current.

The evolution of the CDW phase when current is increased can be seen as an anharmonic to harmonic transition, as it gets closer to a pure sine function. This kind of transition has been observed in many fields of condensed matter, especially in incommensurate molecular crystals,[24] liquid crystals in the smectic phase,[25] or magnetic systems.[26,27] The anharmonicity is particularly visible by neutron and x-ray diffraction since it leads to an increase of the higher-order satellites intensity. In all these examples, the anharmonicity appears when temperature is decreased. In our case, an analogy can be done considering the velocity instead of the temperature.

As a conclusion, we report in this paper on the structural study of the current-driven CDW in blue bronze. An extra modulation appears at I_T and is interpreted as the formation of a soliton lattice. Its period decreases with current, until saturation at 4 mA. Above this current, the soliton lattice has the same correlation length as the CDW itself, and the long-range periodicity is stabilized. The description proposed here is an alternative to the discommensuration model but a theoretical justification still has to be found to clarify the mechanism responsible for the change of periodicity with current.

The authors acknowledge J. Marcus for providing us with the sample, and N. Kirova for helpful discussions.

*vjacques@esrf.fr

[1] P. Monceau *et al.*, Phys. Rev. Lett. **37**, 602 (1976).
[2] P. A. Lee, T. M. Rice, and P. W. Anderson, Solid State Commun. **14**, 703 (1974).
[3] J. B. Sokoloff, Phys. Rev. B **16**, 3367 (1977).
[4] C. Schlenker *et al.*, in *Low-Dimensional Electronic Properties of Molybdenum Bronzes and Oxides*, edited by C. Schlenker (Kluwer, Dordrecht, 1989), p. 159.
[5] T. Tamegai *et al.*, Solid State Commun. **51**, 585 (1984).
[6] R. M. Fleming, R. G. Dunn, and L. F. Schneemeyer, Phys. Rev. B **31**, 4099 (1985).
[7] R. Danneau, A. Ayari, D. Rideau, H. Requardt, J. E. Lorenzo, L. Ortega, P. Monceau, R. Currat, and G. Grubel, Phys. Rev. Lett. **89**, 106404 (2002).
[8] D. DiCarlo, E. Sweetland, M. Sutton, J. D. Brock, and R. E. Thorne, Phys. Rev. Lett. **70**, 845 (1993).
[9] H. Requardt, F. Y. Nad, P. Monceau, R. Currat, J. E. Lorenzo, S. Brazovskii, N. Kirova, G. Grubel, and C. Vettier, Phys. Rev. Lett. **80**, 5631 (1998).
[10] Y. Li, S. G. Lemay, J. H. Price, K. Cicak, K. ONeill, K. Ringland, K. D. Finkelstein, J. D. Brock, and R. E. Thorne, Phys. Rev. Lett. **83**, 3514 (1999).
[11] A. F. Isakovic, P. G. Evans, J. Kmetko, K. Cicak, Z. Cai, B. Lai, and R. E. Thorne, Phys. Rev. Lett. **96**, 046401 (2006).
[12] D. LeBolloch, V. L. R. Jacques, N. Kirova, J. Dumas, S. Ravy, J. Marcus, and F. Livet, Phys. Rev. Lett. **100**, 096403 (2008).
[13] L. Paolasini *et al.*, J. Synchrotron Radiat. **14**, 301 (2007).
[14] F. Livet, Acta Crystallogr., Sect. A **63**, 87 (2007).
[15] M. Greenblatt, in *Low-Dimensional Electronic Properties of Molybdenum Bronzes and Oxides* (Ref. 4), p. 1.
[16] J.-L. Mozos, P. Ordejón, and E. Canadell, Phys. Rev. B **65**, 233105 (2002).
[17] J. Dumas, C. Schlenker, J. Marcus, and R. Buder, Phys. Rev. Lett. **50**, 757 (1983).
[18] D. Feinberg and J. Friedel, in *Low-Dimensional Electronic Properties of Molybdenum Bronzes and Oxides* (Ref. 4), p. 407.
[19] D. LeBolloch, S. Ravy, J. Dumas, J. Marcus, F. Livet, C. Detlefs, F. Yakhou, and L. Paolasini, Phys. Rev. Lett. **95**, 116401 (2005).
[20] J. Dumas, B. Laayadi, and R. Buder, Phys. Rev. B **40**, 2968 (1989).
[21] W. L. McMillan, Phys. Rev. B **14**, 1496 (1976).
[22] S. Brazovskii and T. Nattermann, Adv. Phys. **53**, 177 (2004).
[23] P. Bak, Rep. Prog. Phys. **45**, 587 (1982).
[24] R. Blinc, *Incommensurate Phases in Dielectrics* (North-Holland, Amsterdam, 1986).
[25] L. Noirez *et al.*, Liq. Crystallogr. **16**, 1081 (1994).
[26] M. A. SalgueirodaSilva, J. B. Sousa, B. Chevalier, J. Etourneau, E. Gmelin, and W. Schnelle, Phys. Rev. B **52**, 12849 (1995).
[27] S. Tencé *et al.*, J. Phys.: Condens. Matter **20**, 255239 (2008).
[28] J.-P. Pouget, in *Low-Dimensional Electronic Properties of Molybdenum Bronzes and Oxides* (Ref. 4), p. 87.